Eur. Phys. J. B **61**, 59–66 (2008)
DOI: 10.1140/epjb/e2008-00040-2

THE EUROPEAN PHYSICAL JOURNAL B

Low-field magnetic response of multi-junction superconducting quantum interference devices

R. De Luca[a] and A. Fedullo

DMI, Università degli Studi di Salerno, Via Ponte Don Melillo, 84084 Fisciano (SA), Italy

Received 15 November 2007
Published online 31 January 2008 –

Abstract. The magnetic states of multi-junction superconducting quantum interference device containing $2N$ identical conventional Josephson junctions are studied by means of a perturbation analysis of the non-linear first-order ordinary differential equations governing the dynamics of the Josephson junctions in these devices. In the zero-voltage state, persistent currents are calculated in terms of the externally applied magnetic flux Φ_{ex}. The resulting d.c. susceptibility curves show that paramagnetic and diamagnetic states are present, depending on the value of Φ_{ex}. The stability of these states is qualitatively studied by means of the effective potential notion for the system.

PACS. 74.50.+r Tunneling phenomena; point contacts, weak links, Josephson effects – 85.25.Dq Superconducting quantum interference devices (SQUIDs)

1 Introduction

Ordinary d.c. SQUIDs (Superconducting QUantum Interference Devices) and π-SQUIDs are interesting dynamical systems both for their actual and potential applications [1–3] and for the richness of their dynamical properties [4]. Lately, π-SQUIDs have been proposed as elementary memory devices in quantum computing applications [5], while asymmetric d.c. SQUIDs have been shown to possess a ratchet-like potential, which gives rise to voltage rectification [6]. Multi-junction superconducting devices, on the other hand, can be adopted as model systems in studying the magnetic response of granular superconductors [7–9].

In most of the above applications and basic studies, the exact knowledge of the magnetic metastable states of this system is of great importance. Therefore, when the nature of the so-called paramagnetic Meissner effect (PME) in granular superconductors is to be investigated by means of models whose basic elements are loops containing Josephson junctions [10], detailed studies of the electrodynamic properties of multi-junction quantum interferometer models might be useful. In these systems, the magnetic states can be characterized by the sign of the persistent current, which, in turn, is seen to depend upon the applied magnetic flux Φ_{ex}.

Recently, d.c. SQUID properties have been studied by means of reduced models arising from a perturbation approach to the analysis of the complete set of dynamical equations for the gauge-invariant superconducting phase differences across the Josephson junctions [4–11]. To zero order in the SQUID parameter β (i.e., in the limit of $\beta = 0$) the model does not allow discussion of the magnetic states of the superconducting system. Nevertheless, the $\beta = 0$ approximation for SQUID systems is widely used in the literature when the electrodynamic properties, such as voltage-current characteristics and critical current and time average voltage versus applied magnetic flux curves, are to be interpreted [1–3]. The lowest degree of approximation in β allowing analytical determination of the magnetic states of the superconducting quantum interference devices is given by the first order perturbation solutions of the model equations. By this approach it is possible to determine the d.c. susceptibility and the persistent currents circulating in the system in terms of the externally applied magnetic flux Φ_{ex} [12].

In the present work we determine the magnetic states of a multi-junction symmetric (equal branch inductance) superconducting quantum interference device containing N identical (same coupling and resistive parameters) overdamped conventional Josephson junctions in each branch, by generalizing the results obtained for a conventional symmetric quantum interferometer containing two identical junctions.

The paper is thus organized as follows. In the next section we derive the dynamical equation for a multi-junction interference device containing $2N$ identical Josephson junctions. In the third section, the persistent currents of these devices is calculated in terms of the externally applied flux Φ_{ex}. In the fourth section, by also finding the d.c. magnetic susceptibility as a function of Φ_{ex}, it is shown that the system may present either paramagnetic, either

[a] e-mail: rdeluca@unisa.it

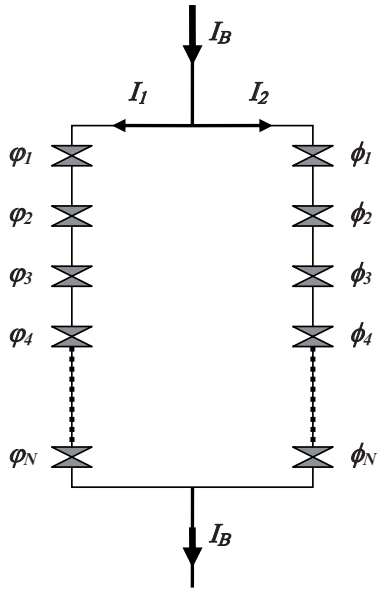

Fig. 1. Schematic representation of a multi-junction quantum interferometer with $2N$ junctions.

diamagnetic states. The nature of these magnetic states is discussed in the fifth section, by finding the effective potential of the system. Conclusions are drawn in the last section.

2 The dynamical equations

In the present section we shall derive an approximate analytic expression for the dynamical equation of a multi-junction quantum interference device containing, on each of the two symmetric branches, N identical point-like overdamped Josephson junction, with resistive and coupling parameters R and I_J, respectively. As shown in Figure 1, the gauge-invariant superconducting phase differences across the JJs on the left branch and on the right branch of the device are denoted as φ_k and ϕ_k ($k = 1, 2, ..., N$), respectively. A bias current I_B is injected in the system, splitting into the two branch currents I_1 (left branch) and I_2 (right branch), so that: $I_B = I_1 + I_2$. Since the same current flows trough all JJs on each branch, and given that all JJs are considered as perfectly identical, we may consider phase locked states, for which

$$\varphi_1 = \varphi_2 = ... = \varphi_N = \varphi, \tag{1a}$$

$$\phi_1 = \phi_2 = ... = \phi_N = \phi. \tag{1b}$$

Because of symmetry, the same inductance L pertains to both superconducting branches, so that we may set $\beta = \frac{LI_J}{\Phi_0}$, Φ_0 being the elementary flux quantum. Let us also define the following normalized quantities: $i_1 = \frac{I_1}{I_J}$ and $i_2 = \frac{I_2}{I_J}$ (normalized branch currents) and $\Psi_{ex} = \frac{\Phi_{ex}}{\Phi_0}$ (normalized applied flux). By setting the total flux linked to the superconducting loop equal to the sum of the externally applied flux Φ_{ex} and of the induced flux, we have, in normalized form:

$$\Psi = \Psi_{ex} + \beta\,(i_1 - i_2)\,. \tag{2}$$

By fluxoid quantization, considering equation (1), we may write:

$$\varphi - \phi + \frac{2\pi}{N}\Psi = 2\pi\frac{n}{N} \tag{3}$$

where n is an integer. With the aid of the RSJ model for the overdamped Josephson junctions in the device and in the absence of noise, the dynamical equations for the variables φ and ϕ can be written as follows [1]:

$$\frac{d\varphi}{d\tau} + \sin\varphi = i_1, \tag{4a}$$

$$\frac{d\phi}{d\tau} + \sin\phi = i_2, \tag{4b}$$

where $\tau = \frac{2\pi RI_J}{\Phi_0}t$ is a normalized time. By means of equation (2) and of the charge conservation relation $i_B = i_1 + i_2$, we may express the currents i_1 and i_2 in terms of the fluxes Ψ and Ψ_{ex}, so that equations (4a-b) become:

$$\frac{d\varphi}{d\tau} + \sin\varphi - \frac{\Psi}{2\beta} = \frac{i_B}{2} - \frac{\Psi_{ex}}{2\beta}, \tag{5a}$$

$$\frac{d\phi}{d\tau} + \sin\phi + \frac{\Psi}{2\beta} = \frac{i_B}{2} + \frac{\Psi_{ex}}{2\beta}. \tag{5b}$$

By fluxoid quantization, expressed in equation (3), equations (5a-b) can be written in terms of two more convenient variables $\varphi_A = \frac{\varphi+\phi}{2}$ and $\xi = \frac{\phi-\varphi}{2\pi} = \frac{\Psi-n}{N}$. In this way, we have:

$$\frac{d\varphi_A}{d\tau} + \cos(\pi\xi)\sin\varphi_A = \frac{i_B}{2}, \tag{6a}$$

$$\pi\frac{d\xi}{d\tau} + \sin(\pi\xi)\cos\varphi_A + \frac{N\xi}{2\beta} = \frac{\Psi_{ex} - n}{2\beta}. \tag{6b}$$

Notice that, by setting $\tilde{\beta} = \frac{\beta}{N}$ and $\tilde{\Psi}_{ex} = \frac{\Psi_{ex}-n}{N}$, equations (6a-b) are formally identical to the dynamical equations for a SQUID, written in terms of the average phase difference φ_A and the fluxon number ξ.

This analogy will allow us to make use of already known results on d.c. SQUIDs. By considering the applied magnetic flux constant and the phase time evolution to be much slower than the fluxon dynamics within the loop [13], we may look for a first-order perturbed solution $\xi(\tau)$ to equation (6b) of the type:

$$\xi(\tau) = \tilde{\Psi}_{ex} + \tilde{\beta}\xi_1(\tau)\,, \tag{7}$$

where, as specified above, $\tilde{\beta} = \frac{\beta}{N}$ and $\tilde{\Psi}_{ex} = \frac{\Psi_{ex}-n}{N}$. By substituting equation (7) into equation (6b), we find, to first order in $\tilde{\beta}$:

$$\xi(\tau) = \tilde{\Psi}_{ex} - 2\tilde{\beta}\sin\left(\pi\tilde{\Psi}_{ex}\right)\cos\varphi_A. \tag{8}$$

$$\begin{aligned}
&\bar{\varphi}_A = 0 \text{ for } x > \sqrt{1+\left(\tfrac{1}{4\pi\tilde{\beta}}\right)^2} - \tfrac{1}{4\pi\tilde{\beta}};\\
&\text{both } \bar{\varphi}_A = 0 \text{ and } \bar{\varphi}_A = \pi \text{ for } -\left(\sqrt{1+\left(\tfrac{1}{4\pi\tilde{\beta}}\right)^2} - \tfrac{1}{4\pi\tilde{\beta}}\right) < x < \left(\sqrt{1+\left(\tfrac{1}{4\pi\tilde{\beta}}\right)^2} - \tfrac{1}{4\pi\tilde{\beta}}\right);\\
&\bar{\varphi}_A = \pm\pi \text{ for } x < -\left[\sqrt{1+\left(\tfrac{1}{4\pi\tilde{\beta}}\right)^2} - \tfrac{1}{4\pi\tilde{\beta}}\right].
\end{aligned} \tag{13}$$

$$i_S = \begin{cases}
-2y \text{ for } x > \sqrt{1+\left(\tfrac{1}{4\pi\tilde{\beta}}\right)^2} - \tfrac{1}{4\pi\tilde{\beta}};\\
\text{both } -2y \text{ and } +2y \text{ for } -\left(\sqrt{1+\left(\tfrac{1}{4\pi\tilde{\beta}}\right)^2} - \tfrac{1}{4\pi\tilde{\beta}}\right) < x < \left(\sqrt{1+\left(\tfrac{1}{4\pi\tilde{\beta}}\right)^2} - \tfrac{1}{4\pi\tilde{\beta}}\right);\\
+2y \text{ for } x < -\left[\sqrt{1+\left(\tfrac{1}{4\pi\tilde{\beta}}\right)^2} - \tfrac{1}{4\pi\tilde{\beta}}\right].
\end{cases} \tag{14}$$

This expression, when substituted in equation (6a) gives:

$$\frac{d\varphi_A}{d\tau} + \cos\left(\pi\tilde{\Psi}_{ex}\right)\sin\varphi_A + \pi\tilde{\beta}\sin^2\left(\pi\tilde{\Psi}_{ex}\right)\sin 2\varphi_A = \frac{i_B}{2}. \tag{9}$$

The above equation is a reduced model for a d.c. SQUID having N overdamped identical junctions in each arm. We notice that the present approach is quantitatively valid [4] for $\beta < \frac{N}{\pi|i_B|}$, or $\tilde{\beta} < \frac{1}{\pi|i_B|}$.

3 Persistent currents

By defining the normalized persistent current i_S, in terms of the stationary solution $\bar{\varphi}_A$ of equation (9), as

$$i_S = i_1 - i_2 = \frac{\left(\xi - \tilde{\Psi}_{ex}\right)}{\tilde{\beta}} \approx -2\sin\left(\pi\tilde{\Psi}_{ex}\right)\cos\bar{\varphi}_A, \tag{10}$$

we shall estimate, by the knowledge of $\bar{\varphi}_A$, the persistent current for given values of $\tilde{\Psi}_{ex}$ and i_B. In this way me may set:

$$\sin\bar{\varphi}_A\left(\cos\left(\pi\tilde{\Psi}_{ex}\right) + 2\pi\tilde{\beta}\sin^2\left(\pi\tilde{\Psi}_{ex}\right)\cos\bar{\varphi}_A\right) = \frac{i_B}{2}. \tag{11}$$

In order to make the notation simpler, in solving equation (11) we make the following substitutions: $x = \cos\left(\pi\tilde{\Psi}_{ex}\right)$, $y = \sin\left(\pi\tilde{\Psi}_{ex}\right)$, and $z = \cos\bar{\varphi}_A$, so that equation (11) can be rewritten in the following way:

$$\sqrt{1-z^2}\left(x + 2\pi\tilde{\beta}y^2 z\right) = \frac{i_B}{2}. \tag{12}$$

For $i_B = 0$, the following solutions of equation (12) for z can be found in interval $[0, 2\pi)$: $z = \pm 1$, or $\cos\bar{\varphi}_A = 0$, $\pm\pi$, if $\frac{|x|}{2\pi\tilde{\beta}y^2} > 1$; $z = \pm 1$, $\cos^{-1}\left(\frac{x}{2\pi\tilde{\beta}y^2}\right)$ and $2\pi - \cos^{-1}\left(\frac{x}{2\pi\tilde{\beta}y^2}\right)$, if $\frac{|x|}{2\pi\tilde{\beta}y^2} < 1$. By choosing only stable solutions, we have:

see equation (13) above

In this way, we can summarize the analytic solution for the permanent current for $i_B = 0$ as follows:

see equation (14) above

Notice that the analytic expression of i_S in equation (14) depends upon the value of n through x. The persistent current described by equation (14) is shown in Figure 2a for $\beta = 0.1$ as a function of the applied flux Ψ_{ex} for null bias current and for $N = 10$ and $n = 0$. In Figure 2b, on the other hand, we chose the same parameters, except for the number of initially trapped fluxons n, which is set equal to 5. We notice that the bistability region for i_S (where both solutions $i_S = \pm 2y$ are present) is a rather small interval in the range chosen, appearing over the external flux interval for which

$$-\left(\sqrt{1+\left(\frac{1}{4\pi\tilde{\beta}}\right)^2} - \frac{1}{4\pi\tilde{\beta}}\right) < x < \left(\sqrt{1+\left(\frac{1}{4\pi\tilde{\beta}}\right)^2} - \frac{1}{4\pi\tilde{\beta}}\right)$$

or, to first order in $\tilde{\beta}$, $-2\pi\tilde{\beta} < x < 2\pi\tilde{\beta}$. Given $\tilde{\beta}$ small, we argue that the bistability region is a very small interval in the vicinities of semi-integer values of $\tilde{\Psi}_{ex}$.

For $i_B \neq 0$, on the other hand, the solutions of equation (12) for z can be found to first order in the parameter $\tilde{\beta}$. In this way, we first square both sides of equation (12), and then solve the resulting approximated cubic equation for z by keeping only terms up to first order in β. Finally, we have:

$$z = \pm\sqrt{1 - \frac{i_B^2}{4x^2}} + \frac{\pi\tilde{\beta}\,y^2 i_B^2}{2x^3}. \tag{15}$$

We may see that the above equation does not allow a real solution for z, if $i_B > 2|x|$, which means that, if the junctions are in the running state, there cannot be any persistent current flow, since the superconducting state of the whole system is destroyed. We now need to correctly distinguish between stable and unstable solutions through phase space representation of equation (9). In order to do this, let us look at Figures 3a and 3b, where the stable

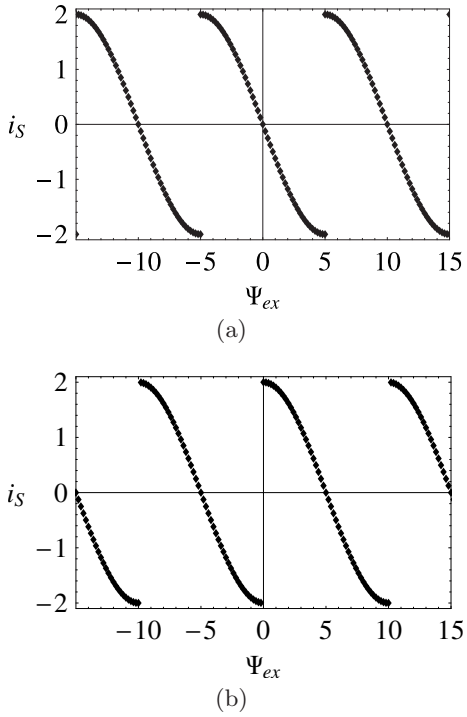

Fig. 2. a) i_S vs. Ψ_{ex} curves for $i_B = 0$, $\beta = 0.1$, $N = 10$ and for $n = 0$. A very small bistability region is present in the vicinities of $\Psi_{ex} = \pm 5$, ± 15, etc. b) i_S vs. Ψ_{ex} curves for $i_B = 0$, $\beta = 0.1$, $N = 10$ and for $n = 5$. The bistability region is now present in the vicinities of $\Psi_{ex} = 0$, ± 10, etc.

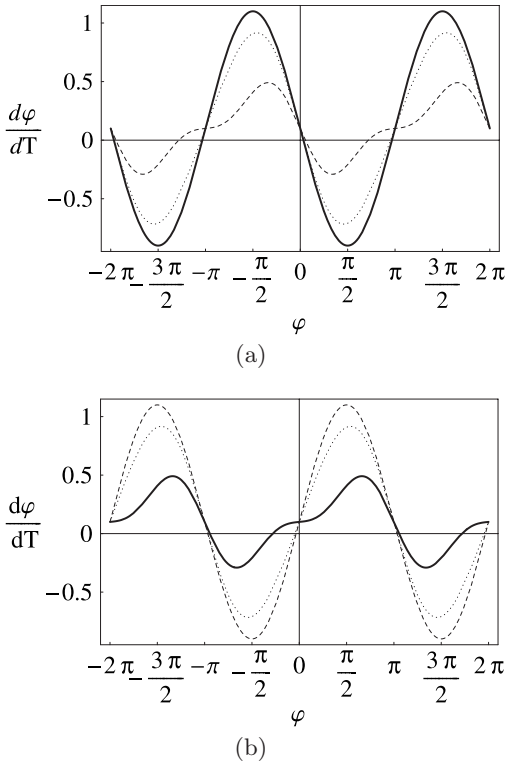

Fig. 3. Phase plane analysis to characterize the stability of fixed points for the reduced model of equation (9) with $N = 10$, $\beta = 0.1$ and $i_B = 0.2$. In Figure 2a we set $\tilde{\Psi}_{ex} = 0$ (full line), $\tilde{\Psi}_{ex} = 0.2$ (dotted line), $\tilde{\Psi}_{ex} = 0.4$ (dashed line). In Figure 2b, instead, we set $\tilde{\Psi}_{ex} = 0.6$ (full line), $\tilde{\Psi}_{ex} = 0.8$ (dotted line), $\tilde{\Psi}_{ex} = 1.0$ (dashed line).

solutions are characterized by the values of $\bar{\varphi}_A$ for which the time derivative goes from positive to negative. As we notice in Figure 3a, where we take $x = \cos\left(\pi\tilde{\Psi}_{ex}\right) > 0$, a stable point is close to the origin. This same point, however, becomes unstable if we take $x = \cos\left(\pi\tilde{\Psi}_{ex}\right) < 0$, as in Figure 3b. In summary, considering the qualitative results in Figures 3a–3b, and noticing that $z = 0$ for $i_B > 2|x|$, we may write:

$$z = \cos\bar{\varphi}_A = \begin{cases} +\sqrt{1-\frac{i_B^2}{4x^2}}+\frac{\pi\tilde{\beta}y^2i_B^2}{2x^3} \text{ if } \frac{i_B}{2} < x \leqslant 1 \\ 0 \text{ if } |x| \leqslant \frac{i_B}{2} \\ -\sqrt{1-\frac{i_B^2}{4x^2}}+\frac{\pi\tilde{\beta}y^2i_B^2}{2x^3} \text{ if } -1 \leqslant x < -\frac{i_B}{2} \end{cases} \tag{16}$$

where we have taken $i_B > 0$ and the instability interval length less than i_B (i.e., to first order in $\tilde{\beta}$, $4\pi\tilde{\beta} < i_B$) for simplicity. Had we considered the instability interval length greater than i_B, some residual bistability would have been present in the system.

Determination of the stable solution given above can be obtained analytically, to first order in $\tilde{\beta}$, in a more rigorous way by considering that the value of the time derivative of φ_A must go from positive to negative, for increasing values of φ_A, in the vicinity of $\bar{\varphi}_A$.

Finally, considering equation (14) and the definition of circulating current given in equation (10), we obtain the following expression for i_S:

$$i_S \approx \begin{cases} -2y\left(\sqrt{1-\frac{i_B^2}{4x^2}}+\frac{\pi\tilde{\beta}y^2i_B^2}{2x^3}\right) \text{ if } \frac{i_B}{2} < x \leqslant 1 \\ 0 \text{ if } |x| \leqslant \frac{i_B}{2} \\ 2y\left(\sqrt{1-\frac{i_B^2}{4x^2}}-\frac{\pi\tilde{\beta}y^2i_B^2}{2x^3}\right) \text{ if } -1 \leqslant x < -\frac{i_B}{2} \end{cases} \tag{17}$$

where, again, we consider $4\pi\tilde{\beta} < i_B$. Representation of the circulating currents is given in Figure 4a for $i_B = 0.2$, $\beta = 0.1$, $N = 10$ and for $n = 0$ (diamonds) and $n = 6$ (stars). A net translation to the right of a quantity $\Psi_{ex} = 6$ is present in the curve with $n = 6$. This properties allows us to argue that the curves with $n = 5$, as shown in Figure 4b, obtained with the same choice of parameters in Figure 4a, have two paramagnetic states, one for positive, one for negative flux values, close to the origin.

These states are characterized by two oppositely circulating persistent currents, which could be attained by letting the field vary from small negative to positive values, or vice versa.

4 Susceptibility

Having derived the persistent currents in the system, the d.c. susceptibility can be readily found. These quantities are of interest in the analysis of the magnetic properties of high temperature superconducting granular systems [14]. The d.c. susceptibility is defined as follows:

$$\chi_{dc} = \frac{\Psi - \Psi_{ex}}{\Psi_{ex}} = \frac{\xi - \tilde{\Psi}_{ex}}{\tilde{\Psi}_{ex} + \frac{n}{N}} = \tilde{\beta}\frac{i_S}{\tilde{\Psi}_{ex} + \frac{n}{N}}. \qquad (18)$$

By the knowledge of i_S from equation (17), we may write, for $4\pi\tilde{\beta} < i_B$:

$$\chi_{dc} \approx \begin{cases} -2\tilde{\beta}\dfrac{y}{\tilde{\Psi}_{ex}+\dfrac{n}{N}}\left(\sqrt{1-\dfrac{i_B^2}{4x^2}}+\dfrac{\pi\tilde{\beta}y^2 i_B^2}{2x^3}\right) & \text{if } \dfrac{i_B}{2} < x \leqslant 1 \\ 0 \text{ if } |x| \leqslant \dfrac{i_B}{2} & \\ 2\tilde{\beta}\dfrac{y}{\tilde{\Psi}_{ex}+\dfrac{n}{N}}\left(\sqrt{1-\dfrac{i_B^2}{4x^2}}-\dfrac{\pi\tilde{\beta}y^2 i_B^2}{2x^3}\right) & \text{if } -1 < x < -\dfrac{i_B}{2}. \end{cases} \qquad (19)$$

Representation of χ_{dc} vs. Ψ_{ex} curves are given in Figures 5a–5b. In particular, in Figure 5a these curves are shown for $i_B = 0.2$, $\beta = 0.1$, $N = 10$ and $n = 0$. In Figure 5b, on the other hand, we show χ_{dc} vs. Ψ_{ex} curves for $i_B = 0.2$, $\beta = 0.1$, $N = 10$ and $n = 5$. Apart from the well known alternate behaviour of the system between diamagnetic and paramagnetic states in Figure 5a ($n = 0$), we notice, in Figure 5b, paramagnetic signals for Ψ_{ex} close to zero, as already noted in the i_S vs. Ψ_{ex} curves for $n = 5$.

5 Effective potential and phase states

In the previous section, by analyzing the i_S vs. Ψ_{ex} curves, we have noticed the presence of two different current states attainable in the vicinities of null applied flux, depending on the sign of Ψ_{ex}. In the same interval, for $i_B = 0$, a bistability region, having amplitude proportional to $\tilde{\beta}$, appears. Therefore, for low values of $\tilde{\beta}$, this region is small. Moreover, it tends to disappear for non-null values of the bias current, as seen in Figures 4a–4b.

In order to qualitatively explain these properties, let us define the Josephson energy of $2N$ Josephson junction as [1]

$$E_J = \frac{\Phi_0 I_J}{2\pi}\left[\sum_{k=1}^{N}(1-\cos\varphi_k) + \sum_{k=1}^{N}(1-\cos\phi_k)\right] = \frac{N\Phi_0 I_J}{2\pi}(2-\cos\varphi-\cos\phi), \qquad (20)$$

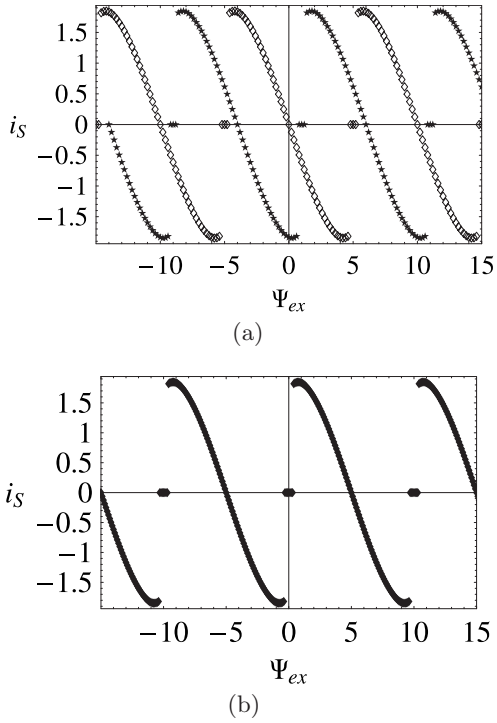

Fig. 4. a) i_S vs. Ψ_{ex} curves for $i_B = 0.2$, $\beta = 0.1$, $N = 10$ and for $n = 0$ (diamonds) and $n = 6$ (stars). A net translation of the second curve to the right of a quantity $\Psi_{ex} = 6$ is detectable. b) i_S vs. Ψ_{ex} curves for $i_B = 0.2$, $\beta = 0.1$, $N = 10$ and for $n = 5$. Notice the existence of two current states in the vicinities of the origin; a positive current state is present at small positive values of Ψ_{ex}, and a negative one, for negative values of Ψ_{ex}.

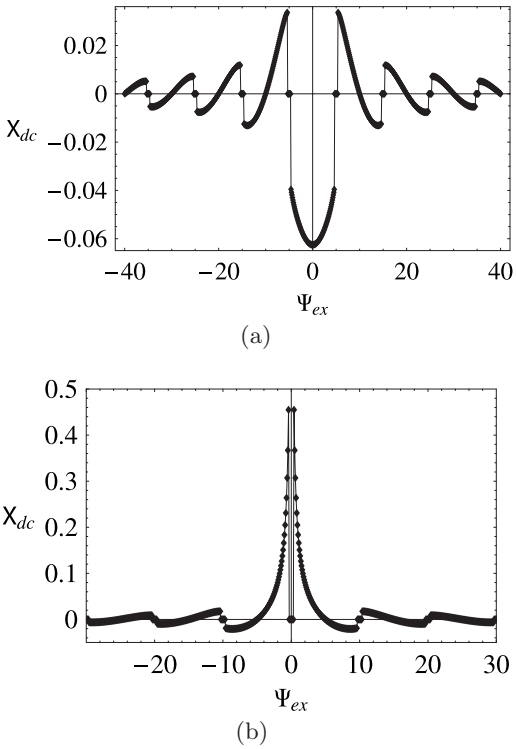

Fig. 5. a) χ_{dc} vs. Ψ_{ex} curves for $i_B = 0.2$, $\beta = 0.1$, $N = 10$ and for $n = 0$. b) χ_{dc} vs. Ψ_{ex} curves for $i_B = 0.2$, $\beta = 0.1$, $N = 10$ and for $n = 5$.

where we have taken, as before, all junctions as perfectly equal. By simple trigonometric identities, we may write:

$$E_J = \frac{N\Phi_0 I_J}{\pi}\left(2 - \cos\varphi_A \cos\pi\xi\right). \tag{21}$$

The electrodynamic potential energy, on the other hand, can be written as follows [1]:

$$\begin{aligned} E_B &= -\frac{\Phi_0 I_J}{2\pi}\left[\sum_{k=1}^{N}\int i_1 d\varphi_k + \sum_{k=1}^{N}\int i_2 d\phi_k\right] \\ &= -\frac{N\Phi_0 I_J}{2\pi}\left[\int i_1 d\varphi + \int i_2 d\phi\right]. \end{aligned} \tag{22}$$

However, by again expressing the variables φ and ϕ in terms of φ_A and ξ, we have:

$$E_B = -\frac{N\Phi_0 I_J}{2\pi}\left[\int i_B d\varphi_A - \pi\int i_S d\xi\right]. \tag{23}$$

By recalling now equation (10), equation (23) takes the following more explicit form:

$$E_B = -\frac{N\Phi_0 I_J}{2\pi}\left[i_B\varphi_A - \pi\frac{\left(\xi - \tilde{\Psi}_{ex}\right)^2}{2\tilde{\beta}}\right], \tag{24}$$

where the first term can be ascribed to the bias current contribution and the second to the applied magnetic flux. By now summing up these two terms, we may write:

$$\begin{aligned} E_{eff} &= E_J + E_B \\ &= \frac{N\Phi_0 I_J}{\pi}\left[2 - \cos\varphi_A\cos\pi\xi - \frac{i_B}{2}\varphi_A + \pi\frac{\left(\xi - \tilde{\Psi}_{ex}\right)^2}{4\tilde{\beta}}\right]. \end{aligned} \tag{25}$$

We can now express the effective energy E_{eff} to first order in the parameter $\tilde{\beta}$, so that, by means of equation (8), we obtain:

$$\begin{aligned} E_{eff} = \frac{N\Phi_0 I_J}{\pi}\Big[&2 - \cos\pi\tilde{\Psi}_{ex}\cos\varphi_A \\ &-\pi\tilde{\beta}\sin^2\pi\tilde{\Psi}_{ex}\cos^2\varphi_A - \frac{i_B}{2}\varphi_A\Big]. \end{aligned} \tag{26}$$

The above expression can be studied for $n = \frac{N}{2}$ (N even), in order to have different current states in the vicinities of $\Psi_{ex} = 0$, as in the example in Section 3. Therefore, by setting $\tilde{\Psi}_{ex} = \frac{\Psi_{ex}}{N} - \frac{1}{2}$, equation (26) becomes

$$\begin{aligned} E_{eff} = \frac{N\Phi_0 I_J}{\pi}\Big[&2 - \sin\left(\pi\frac{\Psi_{ex}}{N}\right)\cos\varphi_A \\ &-\pi\tilde{\beta}\cos^2\left(\pi\frac{\Psi_{ex}}{N}\right)\cos^2\varphi_A - \frac{i_B}{2}\varphi_A\Big]. \end{aligned} \tag{27}$$

The normalized effective energy $e_{eff} = \frac{\pi E_{eff}}{N\Phi_0 I_J}$ is shown, as a function of the average phase difference φ_A, for $\tilde{\beta} = 0.025$ and $N = 4$ in Figures 6a–6c. In Figure 6a, the zero-bias e_{eff} vs. φ_A curves are shown for $\Psi_{ex} = 0.1$ (full line) and $\Psi_{ex} = -0.1$ (dashed line). We notice that, while for small positive values of the normalized applied flux ($\Psi_{ex} = 0.1$), the phase state at $\varphi_A = 0$ is stable, when the field is lowered to $\Psi_{ex} = -0.1$, this state may rapidly decay to phase states $\varphi_A = \pm\pi$. Furthermore, for values of Ψ_{ex} outside the bistability range specified in equation (13), the minima at $\varphi_A = 0$ are not anymore present. However, even though these stable states are present for small negative values of Ψ_{ex} (dashed line in Fig. 6a), given the rather small height of the energy barriers separating this stable state to the adjacent ones ($\varphi_A = \pm\pi$), external noise (as it could be thermal noise or noise due to the applied field or to the bias current) could drive the system out of the $\varphi_A = 0$ state to either one of the stable states $\varphi_A = \pm\pi$, in which the circulating current differs in sign from the initial one (obtained for the phase state $\varphi_A = 0$ at $\Psi_{ex} = 0.1$). In Figure 6b we notice that, by considering all minima in the full-line curve ($i_B = 0$), metastable current states are present, for $\Psi_{ex} = 0.1$, at $\varphi_A = 0$ and in the vicinities of $\varphi_A = \pm\pi$. However, when a small bias current is applied to the system (for example, $i_B = 0.02$, as in the dashed curve of Fig. 6b), the states $\varphi_A = \pm\pi$ rapidly decay to the adjacent ones, a greater probability being associated to the transition to the state on the right. On the other hand, in Figure 6c, where a small negative normalized flux is applied ($\Psi_{ex} = -0.1$), for $i_B = 0$ (full line), we notice that the $\varphi_A = 0$ phase state is short-lived, while the phase states $\varphi_A = \pm\pi$ can be considered to be long-lived with respect to the former. Application of the same small bias current to the system makes it possible to have transitions, in the presence of noise, from the metastable phase state $\varphi_A = 0$ to the adjacent ones ($\varphi_A = \pm\pi$), the highest probability being associated to the transition from $\varphi_A = 0$ to $\varphi_A = \pi$. Higher values of the bias current ($i_B > 4\pi\tilde{\beta}$, to first order in $\tilde{\beta}$) make the short-lived metastable states appearing in both Figures 6b and 6c disappear at all.

For $n = \frac{N}{2}$ (N even) we also exhibit a global view of the potential energy as a function of the average phase difference φ_A and the externally applied flux in Figures 7a–7c for $\tilde{\beta} = 0.025$ and $N = 4$. In particolar, in Figure 7a the bias current is zero, in Figure 7b $i_B = 0.4$ and in Figure 7c $i_B = 0.8$. We notice the appearance of well defined minima in both Figures 7a and 7b, the energy barrier decreasing for i_B increasing from zero to 0.4. These minima are separated by an even smaller energy barrier for $i_B = 0.8$.

In the above we have hypothesized that noise in the system could induce transition from one metastable state to the next; this feature will be studied in details in future work. The characteristic behaviour described above could be promising in the perspective of envisioning a system able to act as a memory cell in quantum computing. As a matter of fact, it can be shown that the above system, which we have essentially described by means of a classical approach, allows extension to a quantum mechanical analysis [15], thus being a candidate for a two-level quantum system useful for realizing quantum computing elementary memory cells. In order to operate this system, we

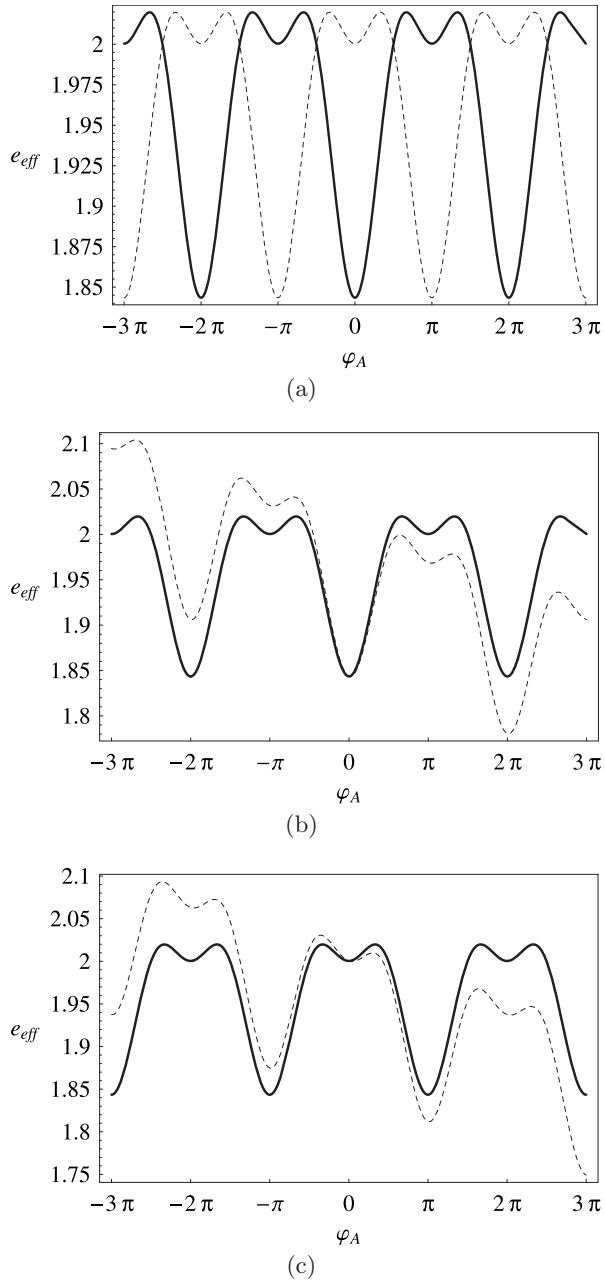

Fig. 6. Effective potential of the quantum interferometer containing $2N$ junctions expressed in terms of the average phase difference φ_A for $\tilde{\beta} = 0.025$ and $N = 4$. a) $i_B = 0.0$, $\Psi_{ex} = +0.1$ (full line) and $\Psi_{ex} = -0.1$ (dashed line). b) $\Psi_{ex} = +0.1$, $i_B = 0.0$ (full line) and $i_B = 0.02$ (dashed line). c) $\Psi_{ex} = -0.1$, $i_B = 0.0$ (full line) and $i_B = 0.02$ (dashed line).

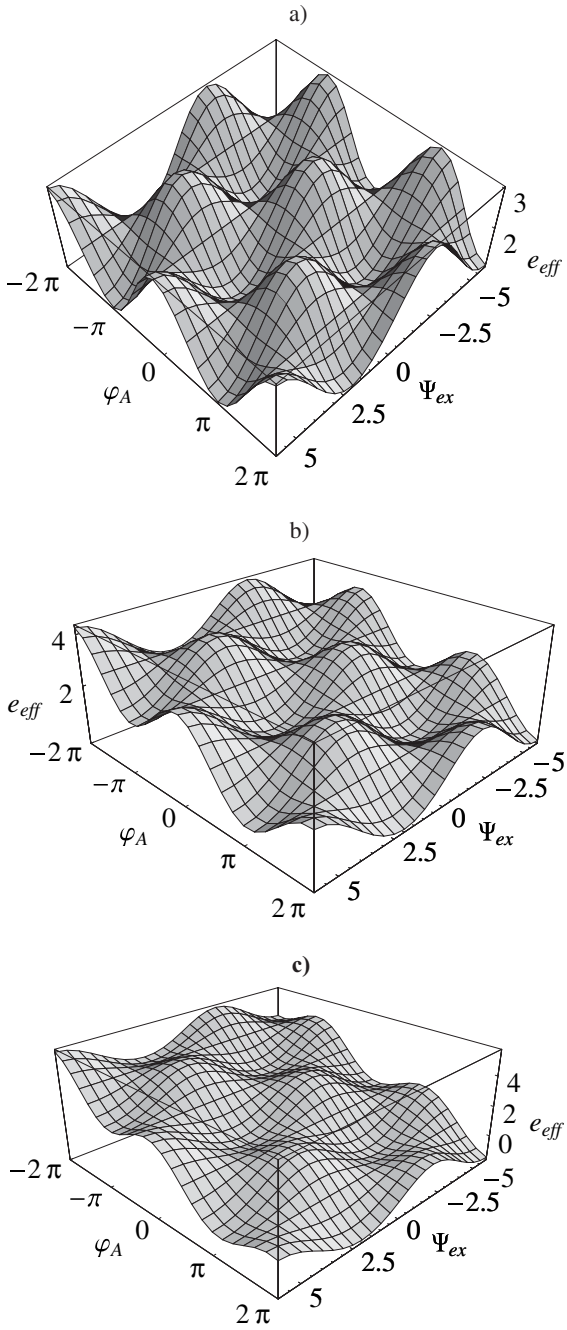

Fig. 7. Effective potential as a function of both the average phase difference φ_A and the externally applied flux Ψ_{ex} for $\tilde{\beta} = 0.025$ and $N = 4$, and for: a) $i_B = 0.0$; b) $i_B = 0.4$; c) $i_B = 0.8$.

can use two external control parameters, the bias current and the externally applied flux. As seen above, both parameters may be used to get transition from one current state to the next, and vice versa.

6 Conclusions

We studied the magnetic states of multi-junction superconducting quantum interference device containing N identical conventional Josephson junctions in each branch. The circulating currents and the d.c. susceptibility have been derived in a closed analytic form by mean of a perturbation analysis of the non-linear first-order ordinary differential equations governing the dynamics of the Josephson junctions. It is shown that the metastable magnetic states can be obtained either by an analytic approach, either by the effective potential notion for the system.

From the d.c. susceptibility curves, the presence of paramagnetic and diamagnetic states, depending on the value of the normalized applied magnetic flux Ψ_{ex}, can be detected. In particular, when the number of trapped fluxons in the system is equal to $\frac{N}{2}$ (N even), two paramagnetic current states of opposite signs are present in the system, one for very small positive values, the other for small negative values of Ψ_{ex}. The stability of all metastable states appearing in this case has been qualitatively studied and possible applications of these devices to quantum computing have been briefly mentioned.

References

1. *The SQUID Handbook*, edited by J. Clarke, A.I. Braginsky (Wiley-VCH, Weinheim, 2004), Vol. I
2. K.K. Likharev, *Dynamics of Josephson Junctions and circuits* (Gordon and Breach, Amsterdam, 1986)
3. A. Barone, G. Paternò, *Physics and Applications of the Josephson Effect* (Wiley, NY, 1982)
4. F. Romeo, R. De Luca, Phys. Lett. A **328**, 330 (2004)
5. T. Yamashita, K. Tanikawa, S. Takahashi, S. Maekawa, Phys. Rev. Lett. **95**, 097001 (2005)
6. I. Zapata, R. Bartussek, F. Sols, P. Hanggi, Phys. Rev. Lett. **77**, 2292 (1996)
7. S.J. Lewandowski, Phys. Rev. B **43**, 7776 (1991)
8. C. Auletta, R. De Luca, S. Pace, G. Raiconi, Phys. Rev. B **47**, 14326 (1993)
9. A. Konopka, S.J. Lewandowski, P.N. Mikheenko, R. Monaco, J. Appl. Phys. **79**, 7871 (1996)
10. P. Barbara, F.M. Araujo-Moreira, A.B. Cawthorne, C.J. Lobb, Phys. Rev. B **60**, 7489 (1999)
11. N. Grønbech-Jensen, D.B. Thompson, M. Cirillo, C. Cosmelli, Phys. Rev. B **67**, 224505 (2003)
12. R. De Luca, F. Romeo, Eur. Phys. J. B **47**, 491 (2005)
13. R. De Luca, A. Fedullo, V.A. Gasanenko, Eur. Phys. J. **B 58**, 461 (2007)
14. W.A.C. Passos, P.N. Lisboa Filho, W.A. Ortiz, Physica C **341–348**, 2723 (2000)
15. F. Romeo, R. De Luca, *Persistent currents in superconducting quantum interference devices*, e-print `arXiv:0704.0546v1 [cond-mat.mes-hall]`